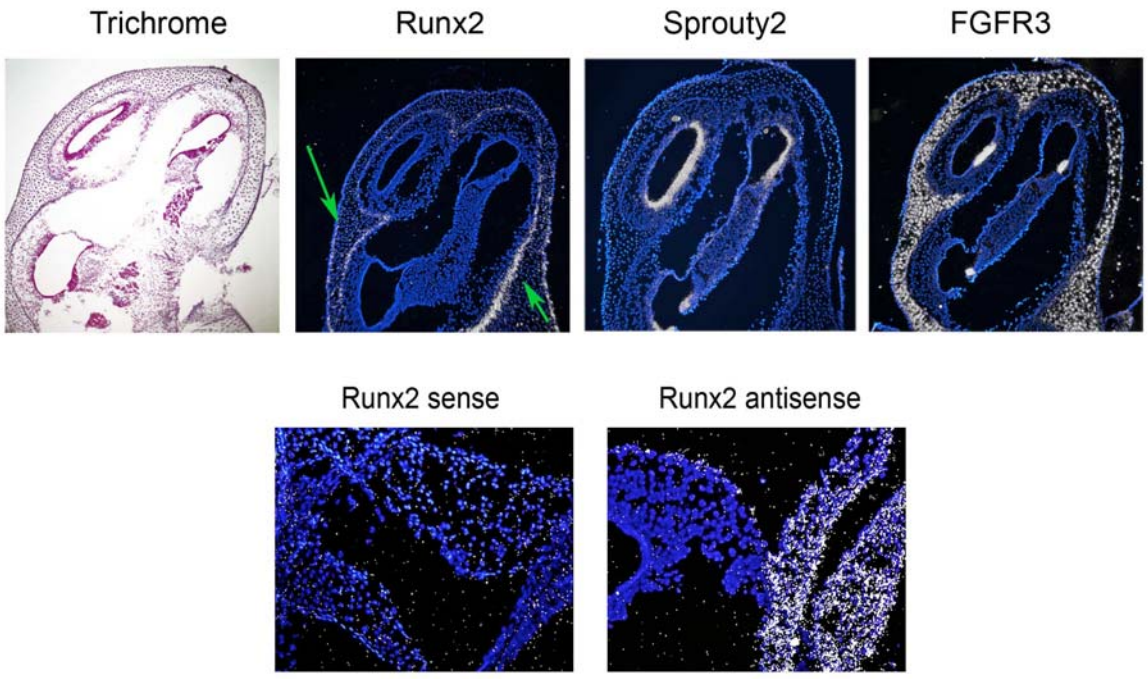


**Figure S1. Runx2 expression localizes to bony, but not sensorineural structures of the cochlea.** In situ hybridization showed that Runx2 (white signal) is expressed only in the developing cochlear capsule at both embryonic day 19 (green arrow) and at postnatal day 21 (data not shown). In contrast, Sprouty2 mRNA was expressed by the developing organ of Corti, whereas fibroblast growth factor receptor 3 was expressed by both bony and sensorineural tissues. These results are consistent with previous data (Shim et al, 2005) and validated the integrity of neural tissues of the cochlea. Together with the lack of signal detected with a sense *Runx2* probe, these results confirmed probe specificity. Importantly, Runx2 was not expressed by cells that give rise to the soft tissues, supporting structures, or neural structures of the cochlea, demonstrating that the consequences of *Runx2* haploinsufficiency were due to an osteoblast-intrinsic defect. Nuclei are counterstained with Hoechst dye (blue).

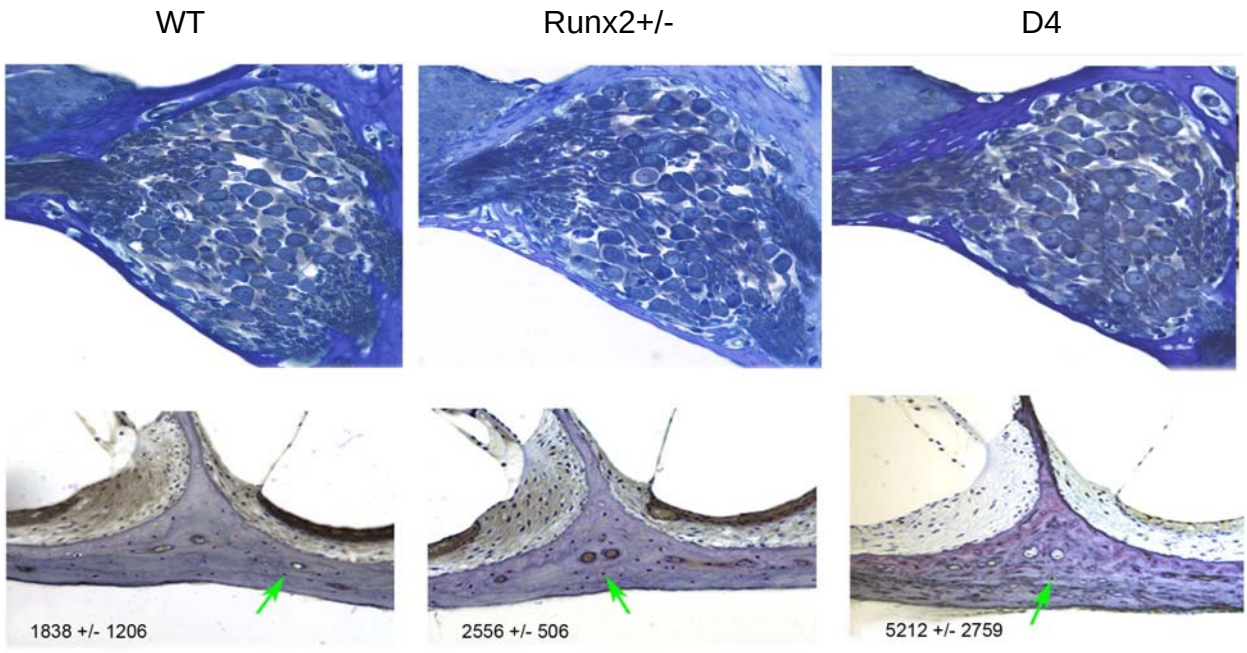


**Figure S2. The cause of CCD-associated hearing loss is not apparent from cochlear histology.** Since compression or atrophy of the eighth cranial nerve causes degeneration of spiral ganglion cells (Sekiya et al, 2000), the qualitatively normal spiral ganglion in *Runx2*$^{+/-}$ and D4 mice (top panels) indicates the integrity of the nerve responsible for hearing. Histologically, the cochlear bone of *Runx2*$^{+/-}$ mice was normal (lower panels). As in D4 femorae (Erlebacher and Derynck, 1996), D4 cochlear bone had increased osteocyte density but this is insufficient to explain HL since *Runx2*$^{+/-}$ mice have normal osteocyte density.

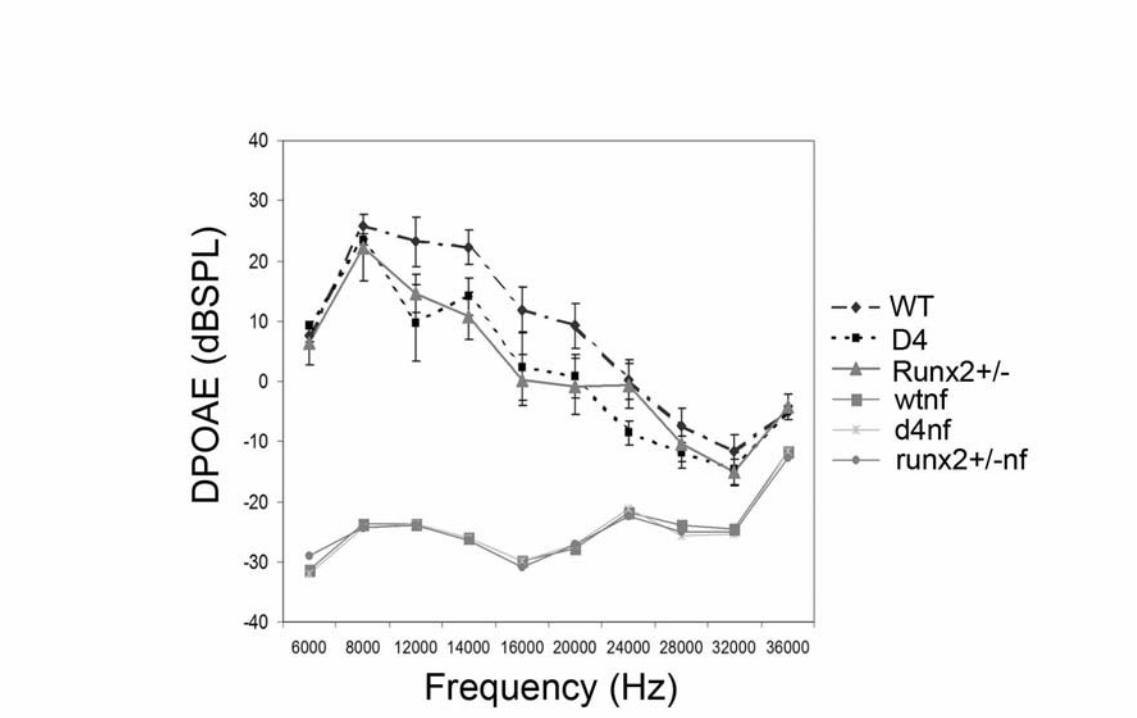


**Figure S3. DPOAE measurements show no significant loss of middle ear function.** To test outer hair cell function, distortion product otoacoustic emissions (DPOAE) were measured in D4, Runx2$^{+/-}$, and wild-type mice. No significant differences among these mouse strains were observed, indicating that outer hair cell function is normal. The noise floor (nf) is indicated for each mouse strain (wtnf, d4nf, runx2+/-nf). Furthermore, since even a slight conductive hearing loss can reduce DPOAEs (Babic et al, 2006), this result localizes at least some of the hearing loss in the D4 and Runx2$^{+/-}$ mice to the cochlea.

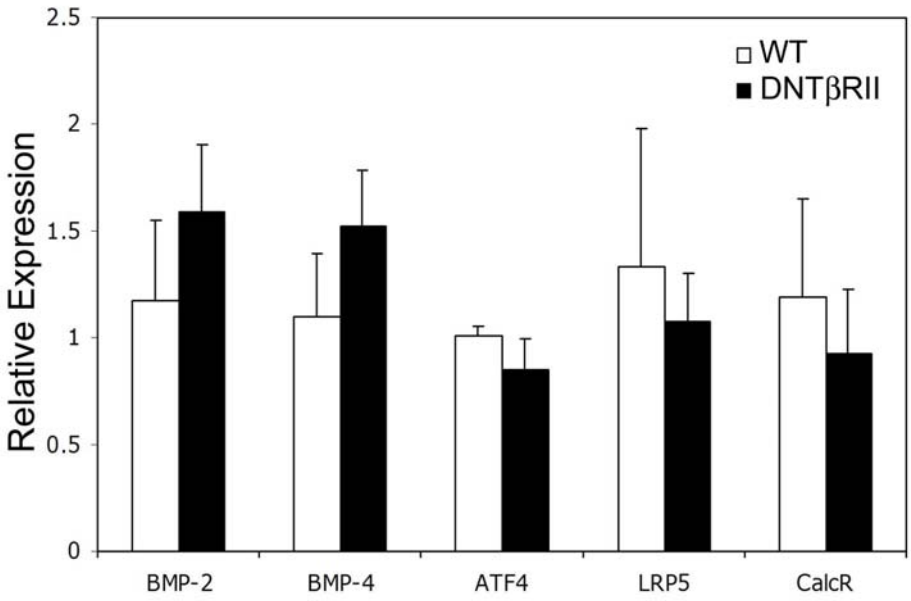


**Figure S4. Several osteoblast gene expression levels in DNTβRII mice are unchanged.** Unlike Runx2, which is significantly induced more than two-fold in bone from DNTβRII mice that express a dominant negative TGF-β type II receptor (Figure 5b), mRNAs for several other regulators of osteoblast differentiation are not differentially expressed. Expression of ligands (BMP-2 and BMP-4), an osteogenic transcription factor (ATF4), and receptors in the Wnt (LRP5) and calcitonin (CalcR) pathways were not significantly different between bone from DNTβRII mice and their wild-type littermates. Osterix expression was highly variable in both wild-type and DNTβRII bone, but also did not exhibit significant differences (data not shown). Results show averages of relative gene expression for five or more mice per genotype. Together these data suggest that differences in bone matrix material properties do not simply reflect the stage of osteoblast differentiation. This is supported by reports showing that other osteoblast regulatory factors do not affect bone material properties (Lane et al, 2003; Mikic et al, 1995). In addition, the gradient of elastic modulus across multiple bones (cochlea > femur > calvaria) does not correspond to a gradient of osteoblast differentiation.

## METHODS

In Situ Hybridization: For in situ hybridization, cochleae from at least 3 mice per time point (embryonic day 19 and postnatal day 21) were perfused through the round window with 4% paraformaldehyde (PFA) in 0.1M phosphate buffered saline at pH 7.4 (PBS), decalcified in 5% EDTA in 0.1M PBS, and used to generate cryosections for in situ hybridization (ISH). Cyrosections were hybridized with radioactive probes for sense and antisense murine Runx2, FGFR3, and Sprouty2 mRNA (Ducy et al, 1997; Ferguson et al, 1999; Shim et al, 2005).

Histology: Cochleae from at least 4 mice per genotype were embedded in Araldite 502 resin for light microscopy with toluidine blue for qualitative analysis of relative spiral ganglion cell size and quantity throughout the cochlea (Akil et al, 2006). Toluidine blue-stained sections were also used to evaluate the cochlear capsule. Cochleae lacunae density was quantified in mid-modiolar sections of cochlear bone. Analysis of 5 non-adjacent sections per ear of two defined regions, the apex and the cochlear outer wall, gave similar results. Lacunae density (lacunae/$mm^2$) was determined by manual counting of lacunae within regions of measured area.

DPOAE Testing: The distortion product otoacoustic emissions (DPOAEs) were measured as described (Akil et al., 2006). Briefly, an acoustic probe placed in the external auditory canal. Stimuli consisted of two primary tones (f1/f2 = 1.25) digitally synthesized at 100kHz using SigGen software. The primary tones with geometric mean (GM) frequencies ranging from 6 to 36kHz, and equal levels (L1=L2=70dBSPL) were

presented via two separate speakers (EC1; Tucker Davis Technologies, Alachua, FL) to the acoustic probe. DPOAE 2f1-f2 responses were recorded using an ER10B+ (Etymotics Research, Elk Grove Village, IL) microphone assembly within the acoustic probe and the TDT BioSig III system. Responses were amplified, digitally sampled at 100kHz, and averaged over 50 discrete spectra. Fast-Fourier transforms were computed from averaged responses. For each stimulus set, DPOAE amplitude level at 2f1-f2 was extracted and sound pressure levels for data points 100Hz above and below the DPOAE frequency were averaged for the noise floor measurements. DPOAE level was plotted as a function of primary tone GM frequency. Statistical differences were calculated using ANOVA with Bonferroni post-hoc test. Data were collected from at least 4 mice of each genotype.

## REFERENCES

Akil O, Chang J, Hiel H, Kong JH, Yi E, Glowatzki E, Lustig LR (2006) Progressive deafness and altered cochlear innervation in knock-out mice lacking prosaposin. *J Neurosci* **26**(50)**:** 13076-13088

Babic BB, Petakov MS, Djukic VB, Ognjanovic SI, Arsovic NA, Isailovic TV, Milovanovic JD, Macut D, Damjanovic SS (2006) Conductive hearing loss in patients with active acromegaly. *Otol Neurotol* **27**(6)**:** 865-870

Ducy P, Zhang R, Geoffroy V, Ridall AL, Karsenty G (1997) Osf2/Cbfa1: a transcriptional activator of osteoblast differentiation. *Cell* **89**(5)**:** 747-754

Erlebacher A, Derynck R (1996) Increased expression of TGF-beta 2 in osteoblasts results in an osteoporosis-like phenotype. *J Cell Biol* **132**(1-2)**:** 195-210

Ferguson C, Alpern E, Miclau T, Helms JA (1999) Does adult fracture repair recapitulate embryonic skeletal formation? *Mech Dev* **87**(1-2)**:** 57-66

Lane NE, Yao W, Kinney JH, Modin G, Balooch M, Wronski TJ (2003) Both hPTH(1-34) and bFGF increase trabecular bone mass in osteopenic rats but they have different effects on trabecular bone architecture. *J Bone Miner Res* **18**(12)**:** 2105-2115

Mikic B, van der Meulen MC, Kingsley DM, Carter DR (1995) Long bone geometry and strength in adult BMP-5 deficient mice. *Bone* **16**(4)**:** 445-454

Sekiya T, Hatayama T, Shimamura N, Suzuki S (2000) An in vivo quantifiable model of cochlear neuronal degeneration induced by central process injury. *Exp Neurol* **161**(2)**:** 490-502

Shim K, Minowada G, Coling DE, Martin GR (2005) Sprouty2, a mouse deafness gene, regulates cell fate decisions in the auditory sensory epithelium by antagonizing FGF signaling. *Dev Cell* **8**(4)**:** 553-564